THEORETICAL AND EXPERIMENTAL STUDIES OF RADIATIVE PROPERTIES OF SUBSTANCES AND THEIR APPLICATIONS TO LASER AND HEAVY ION INERTIAL FUSION .

N. Orlov.

Joint Institute for High Temperature RAS, Moscow

Theoretical background

As known, precise measurements of physical parameters are limited for laser-produced plasma. Therefore, computer codes, which contain

1. Gas dynamics,
2. Photon transport processes,.
3. Equation of state,
4. The radiative opacity,

are used extensively to determine temperature profiles, density profiles and other plasma characteristics within the target thickness [1,2]. The radiative opacity represents an important part of this study.

1. Orzechowski, T. J., Rosen, M. D., Korblum, M. D., Porter J. L., Suter, L. J., Thissen, A. R., Wallace, R. J. (1996). The Rosseland Mean Opacity of a Mixture of Gold and Gadolinium at High Temperatures. *Phys. Rev. Lett*. **77**, pp. 3545-3548.
2. Callachan-Miller, D.& Tabak, M. (2000). Progress in target physics and design for heavy ion fusion. *Physics of Plasmas.* **7**, No. 5, pp. 2083-2091.

The density – functional theory.

In the grand canonical ensemble, the equilibrium electron density provides minimum of the grand potential

$$\Omega = Sp\{\hat{W}(\hat{H} - \mu\hat{N} + \Theta \ln \hat{W})\},$$

where the density matrix has the form

$\hat{W} = \exp\left[-\frac{\hat{H} - \mu\hat{N}}{\Theta}\right] / Sp\left[-\frac{\hat{H} - \mu\hat{N}}{\Theta}\right]$, here Θ is the plasma temperature.

$$\left|\Phi_A\right\rangle = \left|n_1^A, n_2^A, ..., n_k^A, ...\right\rangle, \quad \hat{H}_A = \sum_i \hat{T}_i + \sum_{i<j} v(\vec{r}_i, \vec{r}_j)$$

$$\hat{T}_i = -\frac{1}{2}\Delta_i - \frac{Z}{r_i} + V_{ext}^A(\vec{r}_i) \qquad v(\vec{r}_i, \vec{r}_j) = \frac{1}{\left|\vec{r}_i - \vec{r}_j\right|}$$

$$\hat{H}_A = \sum_{m,n} \left\langle m\left|\hat{T}\right|n\right\rangle a_m^+ a_n + \frac{1}{2}\sum_{k_1,k_2,k_3,k_4} \left\langle k_1 k_2 \left|v\right| k_4 k_3\right\rangle a_{k_1}^+ a_{k_2}^+ a_{k_3} a_{k_4}$$

$$\Omega = \sum_A W_A E_A - \mu \sum_A W_A N_A + \Theta \sum_A W_A \ln W_A$$

The general set of self-consistent field equations that describe the state of the whole ensemble of plasma atoms and ions.

$$\hat{T}_A \Psi_i(\vec{r}_1) + V_A(\vec{r}_1)\Psi_i(\vec{r}_1) - \sum_{j \le K} n_{Aj}^c \int \Psi_j^*(\vec{r}_2) \frac{1}{|\vec{r}_1 - \vec{r}_2|} \Psi_i(\vec{r}_2) d\vec{r}_2 \Psi_j(\vec{r}_1) = \sum_j \lambda_{ij}^A \Psi_j(\vec{r}_1),$$

$$\bar{n}_A^f(\vec{r}, \vec{p}) = \left\{ \exp\left[\frac{1}{\Theta} \left(\frac{p^2}{2} - \frac{Z}{r} + V_A(\vec{r}) + V_{ext}^A(\vec{r}) - \mu \right) \right] + 1 \right\}^{-1}$$

- the unbound electron density in phase space

$$W_A = C g_A \exp\left\{ -\frac{E_A - \mu N_A}{\Theta} \right\},$$

$$\sum_A W_A N_A = Z.$$

Theoretical models of substances at high energy density.

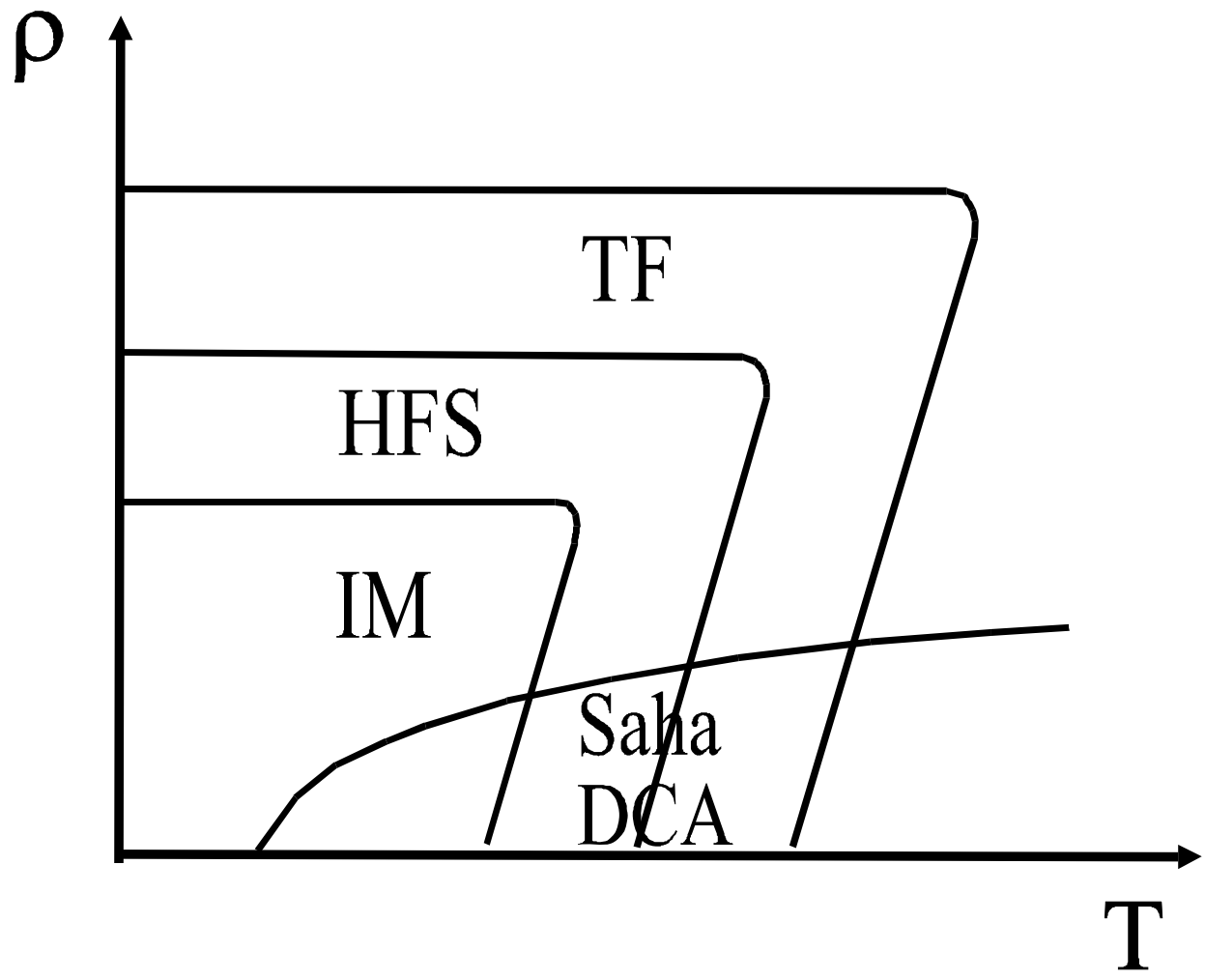

Theoretical models of substances at high energy density.

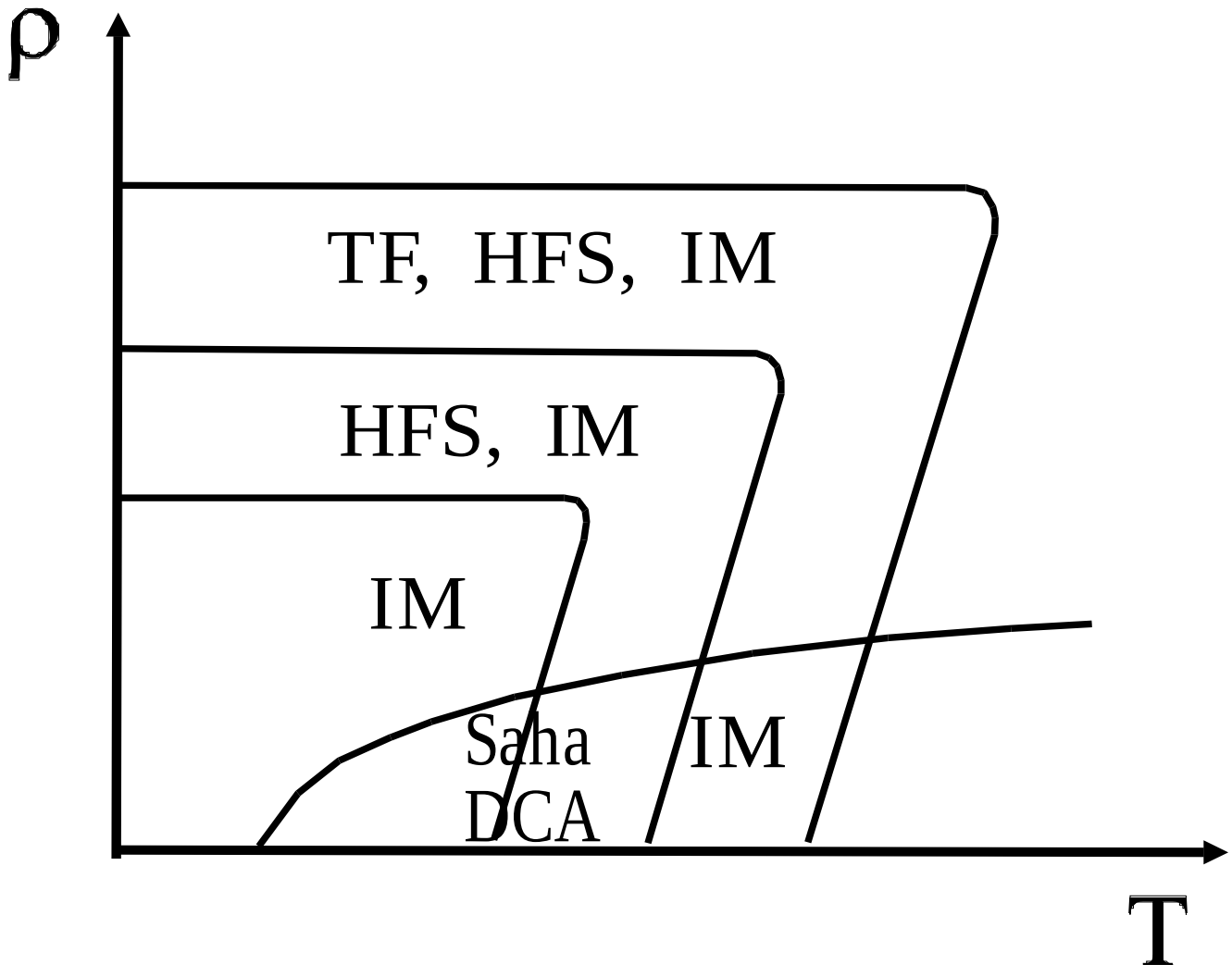

Optically thick plasma.

Optically thick plasma can be produced by laser interaction with a hohlraum wall. It was shown (Orzechowski et al.) that hohlraum wall loss energy ΔE increases proportionally to the square root of the Rosseland mean free path.

$$\Delta E \propto \left[l_R \right]^{1/2} \qquad (1)$$

The hohlraum wall efficiency increases with a reduction of this value. It can be achieved by decreasing the Rosseland mean free path.

Thus, an optimal chemical composition for optically thick plasmas can be achieved by minimizing the Rosseland mean free path.

Optically thin plasma.

Optically thin plasma can be produced by exploding wires. In this case, the outward energy flux increases inversely proportional to the Planck mean free path l_P .

$$j \propto \frac{1}{l_P} \tag{2}$$

The simple formula will be used for estimating relative radiation efficiency of different exploding wires made of two different materials A and B:

$$k = \frac{j^{\mathrm{A}}}{j^{B}} = \frac{l_P^{B}}{l_P^{A}} \tag{3}$$

An optimal chemical composition for optically thin plasmas can be achieved by minimizing the Planck mean free path.

Results of calculations for hohlaum walls.

The spectral coefficient for x-ray absorption was calculated for gold plasma produced by laser interaction with gold hohlraum wall Au (black line). The coefficient for gold is relatively small in the energy interval $(3.5 < x < 8.5)$. The coefficient was also calculated for a composition, which is denoted as Composition 1 (red line). This composition was found using an optimization method. One can see, the interval is overlapped with spectral lines for Composition 1. It provides decreasing the Rosseland mean free path.

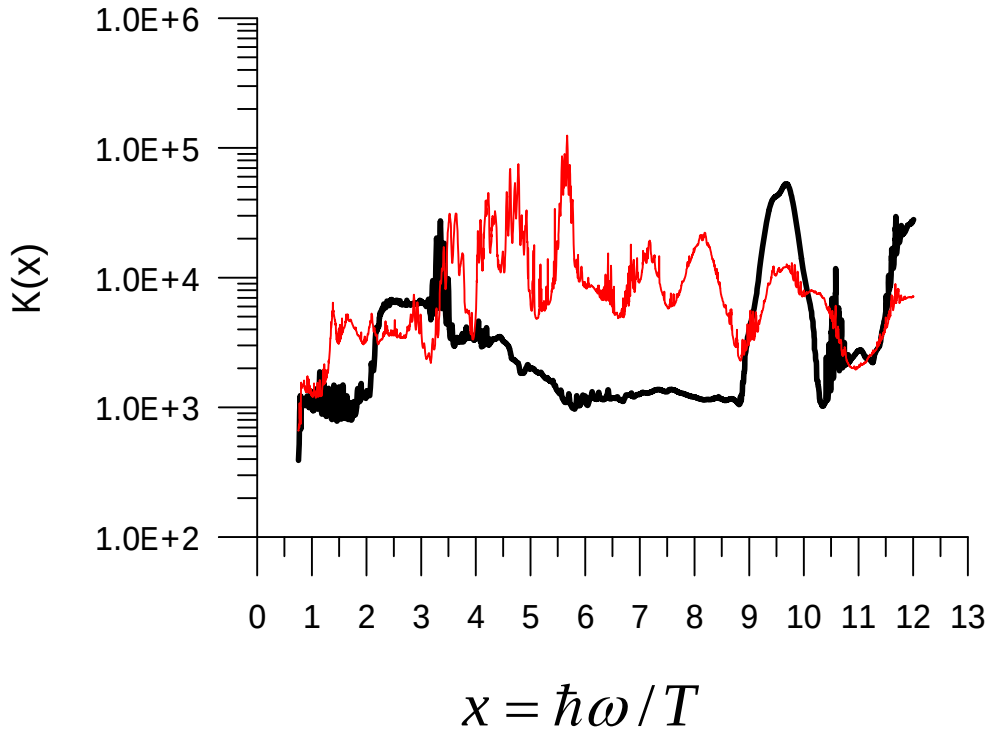

Fig.1 The spectral coefficient for X-rays absorption K(x) (cm^2/g) calculated for Au (black line) and for Composition 1 (Au25.7%/W23.1%/Gd18.1%/Pr10.0%/Ba10.4%/Sb12.7%) (red line) at the temperature T=250 eV and the density $\tilde{\rho} = 1\,\mathrm{g}/cm^3$.

Table 1. The hohlraum wall loss energy for different materials, compared to a Au hohlraum wall $\Delta E_{wall} / \Delta E_{Au}$ and to a AuGd hohlraum wall $\Delta E_{wall} / \Delta E_{AuGd}$.

Au		AuGd	
Material	$\frac{\Delta E_{wall}}{\Delta E_{Au}}$	Material	$\frac{\Delta E_{wall}}{\Delta E_{AuGd}}$
Au	1.00	Au/Gd(50:50)	1.00
Au:Gd	0.83	Au	1.25
U:At:W:Gd:La	0.65	Pb	1.28
U:Bi:W:Gd:La	0.65	W	1.25
U:Bi:Ta:Dy: Nd	0.63	Pb/Ta(70:30)	1.06
Th:Bi:Ta:Sm:Cs	0.68	Hg/Xe(50:50)	1.18
U:Pb:Ta:Dy:Nd	0.63	Pb/Ta/Cs(45:20:35)	1.01
U:Nb.14:Au:Ta:Dy	0.66	Pb/Hf/Xe(45:20:35)	1.00
Comp. 1	0.57	Comp. 1	0.75

Experimental and theoretical study of exploding wires.

The spectral coefficient for x-ray absorption was calculated for NiCr alloy (Ni80%/Cr20%) (black line) and for Alloy 188 (Cr21.72%/Ni22.92%/Fe2.24%/Co39%/ W13.93%) (red line). One can see, the energy interval is overlapped with spectral lines of Alloy 188. It leads to decreasing the Planck mean, and Alloy 188 is more efficient material. Experimental study was carried out to test the theoretical results. Experimental measurements were made for the total energy yield B, and the experimental and theoretical coefficients of relative efficiency can be expressed in the form:

$$k^{exp} = B^{Alloy188} / B^{NiCr} . \qquad k^{theor} = j^{Alloy188} / j^{NiCr}$$

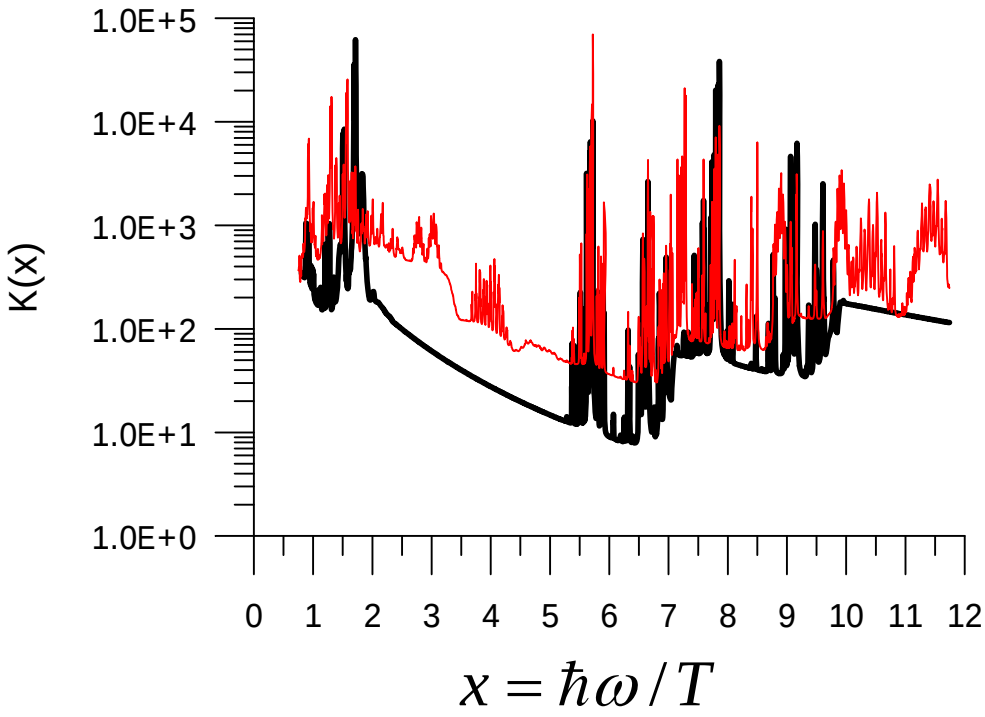

Fig. 2. The spectral coefficient for X-rays absorption K(x) (cm^2/g) calculated for alloy (Ni80%/Cr20%) (black line) and for the composition Alloy 188 (Cr21.72%/Ni22.92%/Fe2.24%/Co39%/W13.93%) (red line) at the temperature T=1 keV and the density $\tilde{\rho} = \tilde{\rho}_{normal}$ **.**

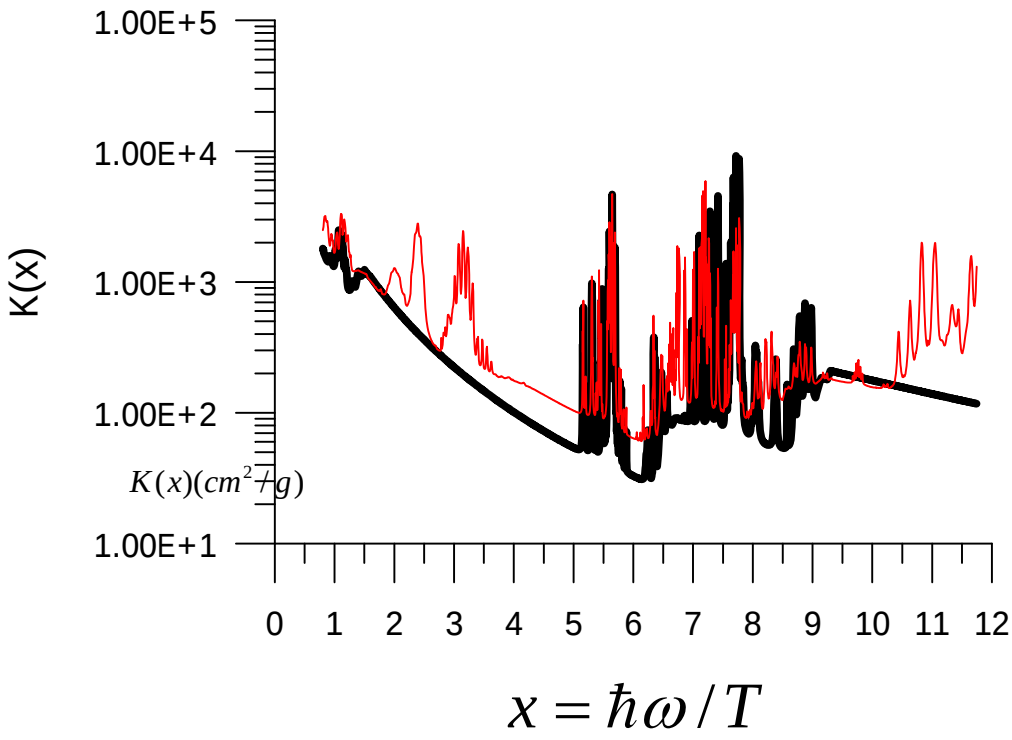

.

Fig. 3. The spectral coefficient of X-rays absorption calculated for NiCr (thick line) and for the composition Alloy 188 (Cr21.72%/Ni22.92%/Fe2.24%/Co39%/W13.93%) (thin line) at the temperature T=1 keV and the density

$$\tilde{\rho} = 10 * \tilde{\rho}_{normal}$$

Experimental and theoretical study of exploding wires.

The spectral coefficient for x-ray absorption was calculated for NiCr alloy (Ni80%/Cr20%) (black line) and for Alloy 188 (Cr21.72%/Ni22.92%/Fe2.24%/Co39%/ W13.93%) (red line). One can see, the energy interval is overlapped with spectral lines of Alloy 188. It leads to decreasing the Planck mean, and Alloy 188 is more efficient material. Experimental study was carried out to test the theoretical results. The total energy yield B was measured using two devices with different energy bands. The experimental and theoretical coefficients of relative efficiency can be expressed in the form:

$$k^{exp} = B^{Alloy188} / B^{NiCr} . \qquad k^{theor} = j^{Alloy188} / j^{NiCr}$$

Table 2. Theoretical and experimental results on the relative radiation energy yield from exploding wires made of alloy (Ni80%/Cr20%) and Alloy 188 (Cr21.72%/Ni22.92%/Fe2.24%/Co39%/ W13.93%).

	Experiment		Theory	
	k^{exp}	Error bar	k^{theor}	$\Delta\%$
(E>1.5 keV)	1.736	20%	1.84	5.6%
(2.5<E<5 keV)	1.9	20%	1.84	3.2%

Symmetric multilayer X-pinch study.

Previous explanations were connected with big differences between the Rosseland or Planck mean free paths for different substances.

A more complicated case is connected with so-called symmetric multilayer X-pinch, where tungsten (W) and molybdenum (Mo) wires are used. Structure of symmetric multilayer X- pinch plasma provides more high radiation efficiency than pure tungsten (Table 3). One of the possible theoretical explanations is connected with specific spectral coefficients for x-ray absorption and radiation.

Structure of symmetric multilayer X- pinch plasma, where tungsten (W) and molybdenum (Mo) wires are used.

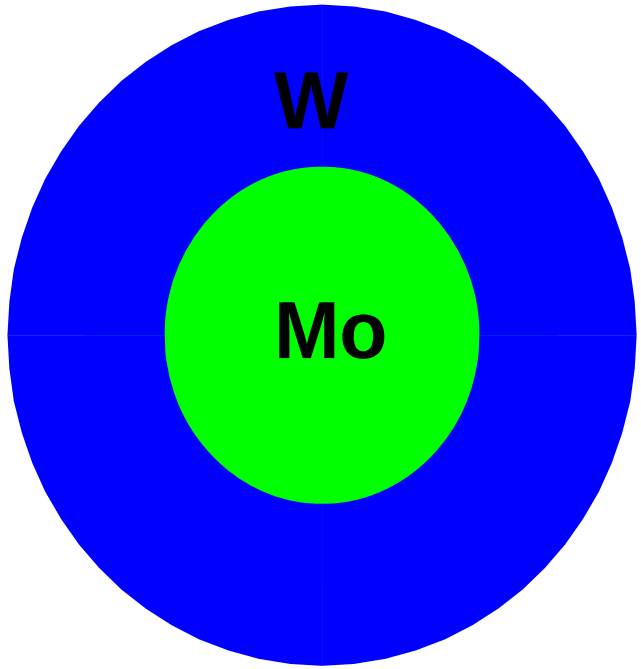

Table 3. Experimental measurements of radiation powers for different X-pinch compositions

X-pinch composition	Radiation power, GW E>1.5 keV	Radiation power, GW 2.5<E<5 keV
W	1.3 ± 0.2	0.4 ± 0.03
(W, Mo)	2.7 ± 0.3	1.2 ± 0.06

Symmetric multilayer X-pinch study. Theoretical explanation.

On the final stage of X- pinch, plasma is compressed up to 10 normal density of initial material. A little range of compressed plasma produces practically all radiation.

The spectral coefficients for x-ray absorption and radiation were calculated for tungsten and molybdenum respectively. One can see, that energy interval of maximal radiation for molybdenum coincides with the interval of maximal absorption for tungsten. Therefore, practically all radiation of molybdenum is absorbed in tungsten.

The effect leads to additional heating or preheating of tungsten plasma. One can note that 20% of additional temperature provides double increasing of radiation yield.

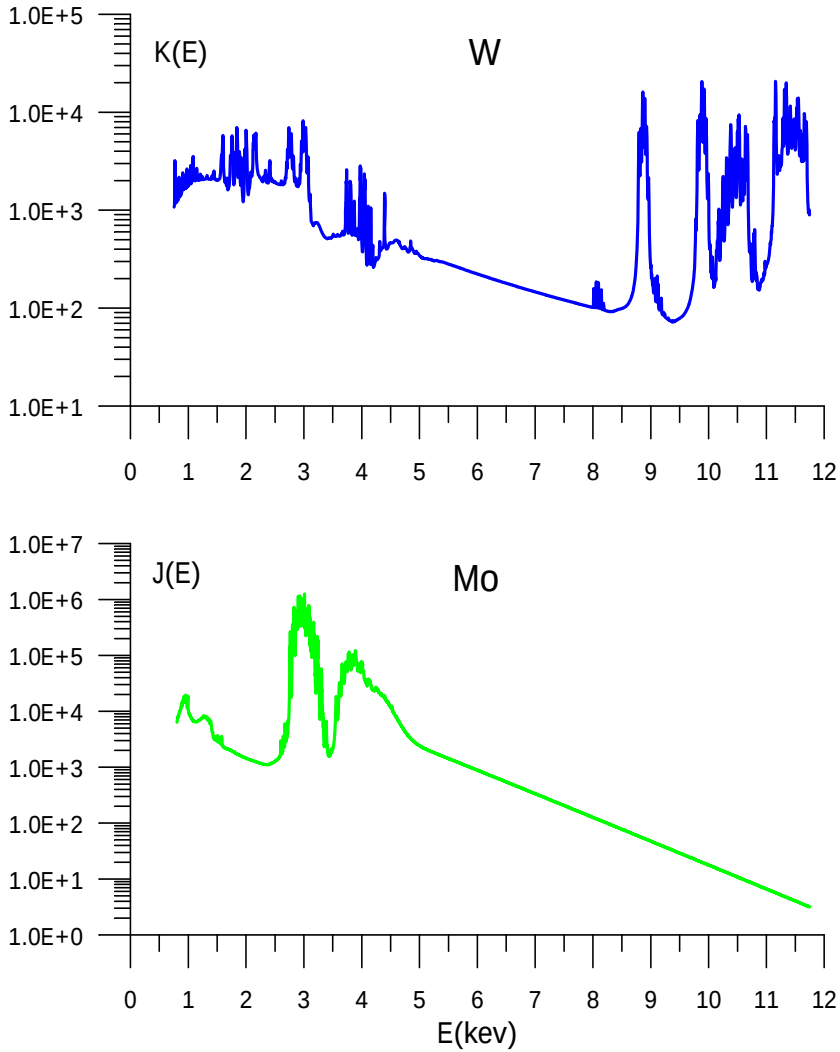

Fig. 4. The spectral coefficient for x-ray absorption K(E) (cm^2/g) calculated for W (blue line) and the spectral coefficient for x-ray radiation J(E) (a.u.) calculated for Mo (green line) at the plasma temperature T=1 keV and normal densities of W and Mo.

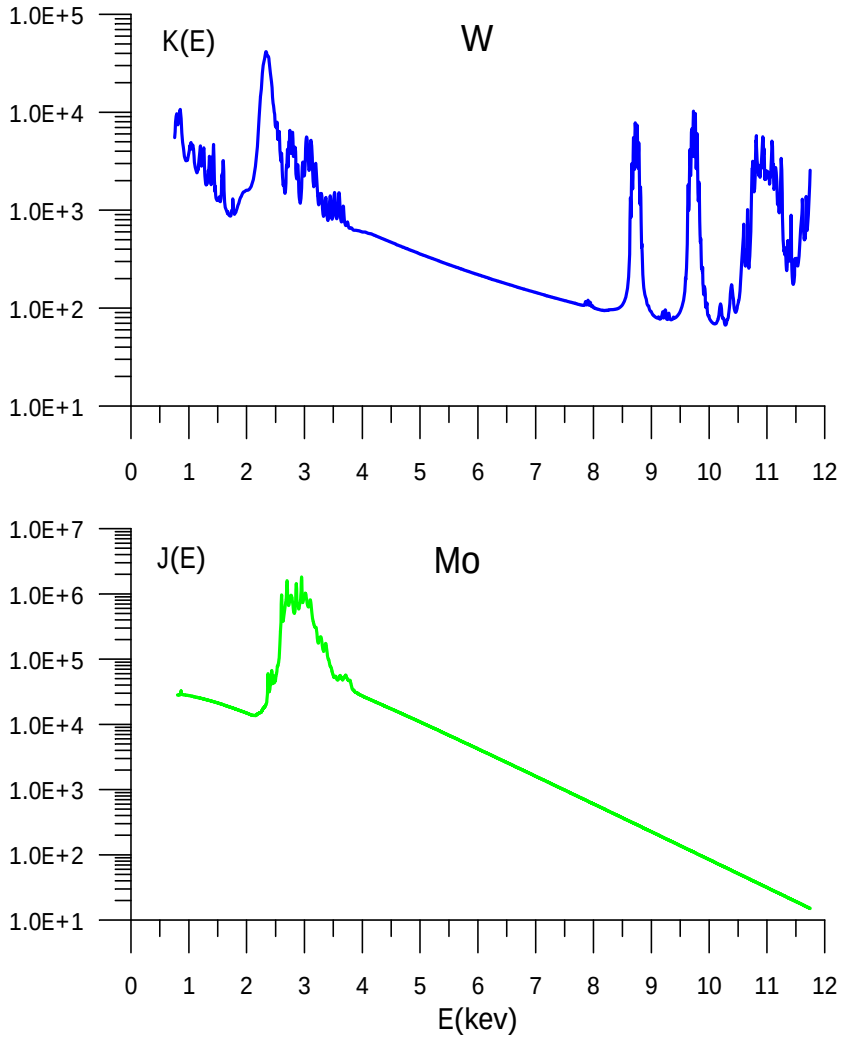

Fig 5. The spectral coefficient for x-ray absorption K(E) (cm2/g) calculated for W (blue line) and the spectral coefficient for x-ray radiation J(E) (a.u.) calculated for Mo (green line) for complex X-pinch at T=1keV and the density $\tilde{\rho} = 10 * \tilde{\rho}_{norm}$

Symmetric multilayer X-pinch study. Theoretical explanation.

On the final stage of X- pinch, plasma is compressed up to 10 normal density of initial material. A little range of compressed plasma produces practically all radiation.

The spectral coefficients for x-ray absorption and radiation were calculated for tungsten and molybdenum respectively. One can see, that energy interval of maximal radiation for molybdenum coincides with the interval of maximal absorption for tungsten. Therefore, practically all radiation of molybdenum is absorbed in tungsten.

The effect leads to additional heating or preheating of tungsten plasma. One can note that 20% of additional temperature provides double increasing of radiation yield.

Diagnostics of the temperature of low Z foams in the combined laser - heavy ion beam experiments.

The theoretical approach can be used for temperature diagnostics of low Z foams in combined laser - heavy ion beam experiments. The experiment needs creating a plasma target, where dense homogeneous plasma can keep the temperature and density during further interaction with heavy-ion beam. Indirect heating of low Z foams with PHELIX-laser pulse can be used to this end.

The temperature diagnostics of CHO-foams can be based on experimental measurements of photo-absorption K-edge energies in carbon. As the temperature increases, the state of the whole ensemble of plasma atoms and ions is changed. It leads to appearance of new ions with more high ionization degree, and states with low ionization vanish. As a result, K-edge energies are considerably changed.

On the other hand, the solution of the general set of self-consistent field equations that describe the state of the whole ensemble of plasma atoms and ions gives, in particular, K-edge energies of different ions in ground and excited states. Comparison of the theoretical and experimental results can be used to determine plasma temperature.

Diagnostics of the temperature of low Z foams in the combined laser - heavy ion beam experiments.

The spectral coefficients for x-ray absorption were calculated at temperatures T=5, 10, 15, 20 eV and the carbon plasma density 0.003 g/cc. The photo-absorption K-edge position is denoted here with corresponding notation, which presents the electron configuration. One can see that K-edge positions are different in dependence on plasma temperature.

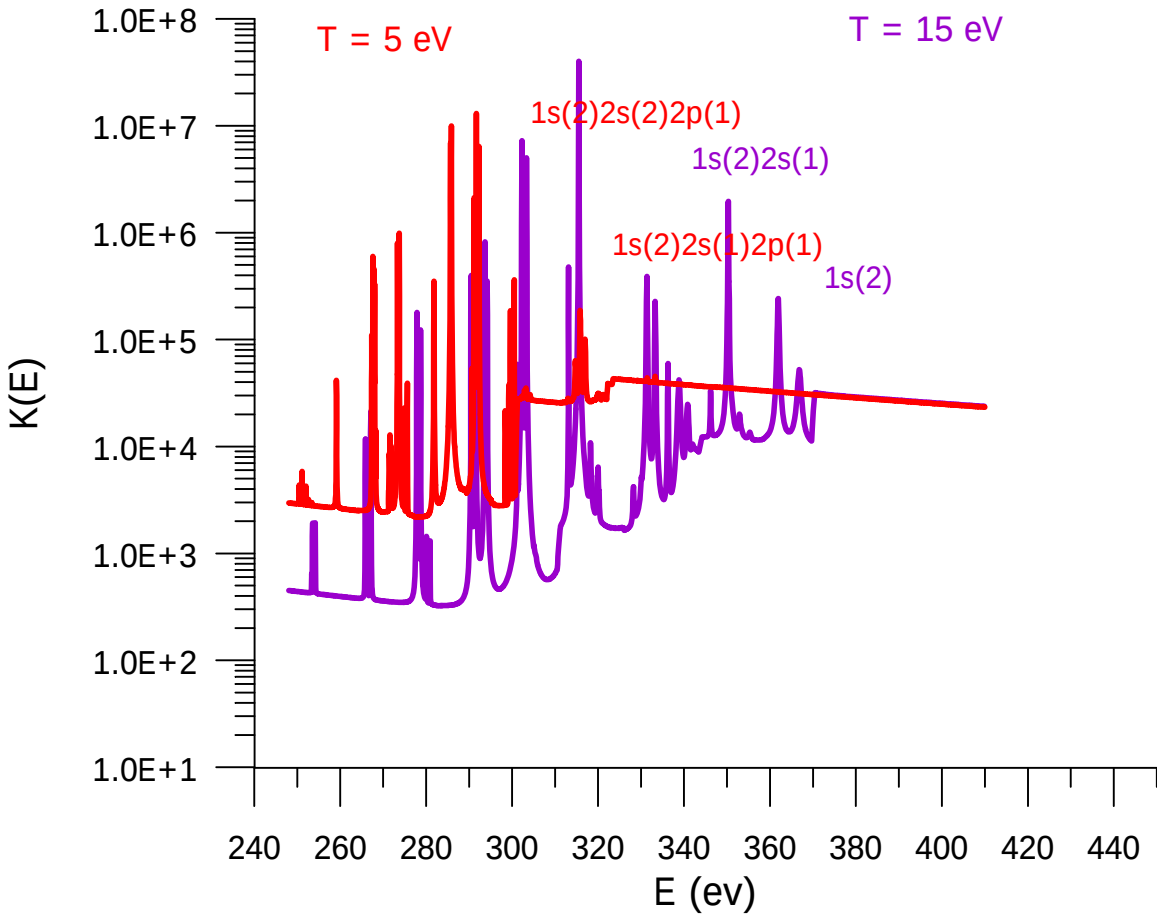

Fig. 6. The spectral coefficient for x-ray absorption K(E) (cm^2/g) calculated for carbon plasma at T=5 eV (red line) and T=15 eV (violet line), and density 0.003 (g/cc).

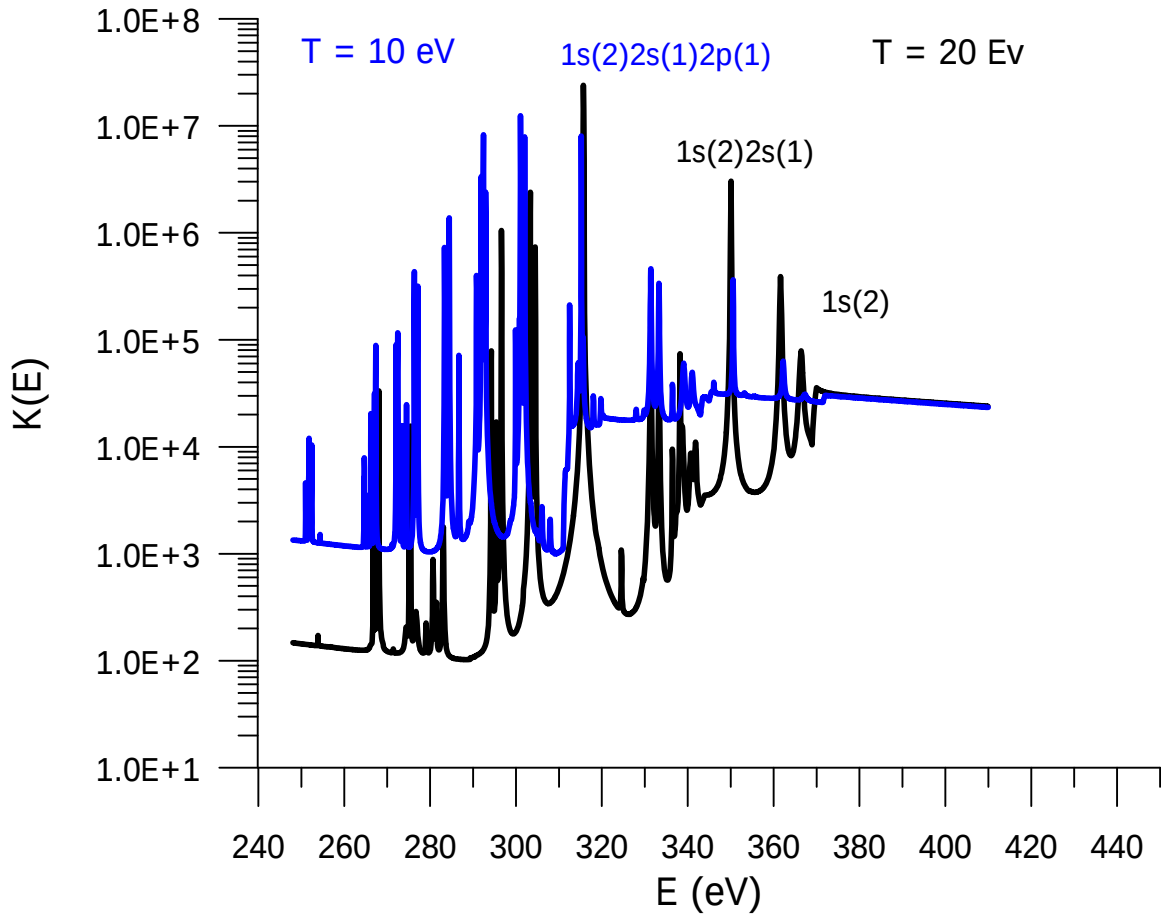

Fig. 7. The spectral coefficient for x-ray absorption K(E) (cm2/g) calculated for carbon plasma at T=10 eV (blue line) and T=20 eV (black line), and plasma density 0.003 (g/cc).

CONCLUSIONS.

1. The Ion Model provides reliable quantum mechanical calculations of radiative opacity over a wide range of plasma temperature and density.
2. The Ion Model can be used to give theoretical explanations of experimental phenomena.
3. The theoretical approach can be used for temperature diagnostics of low Z foams in combined laser - heavy ion beam experiments.

Appendix 1.

Experimental measurements of radiation power for different multilayer X-pinch compositions

X-pinch composition	Radiation power, GW E>1.5 keV	Radiation power, GW 2.5<E<5 keV
W	1.3 ± 0.2	0.4 ± 0.03
(W, Mo)	2.7 ± 0.3	1.2 ± 0.06

Rosseland and Planck mean free paths calculated for W and mixture (W80%Mo20%) at T=1 keV and the density $\tilde{\rho} = 10 * \tilde{\rho}_{norm}$

Composition	Rosseland mean (cm)	Planck mean (cm)
W	1.26 10-5	1.64 10-6
(W80%, Mo20%)	1.49 10-5	1.79 10-6

$k^{exp} = P^{WMo} / P^{W} = 2.08$ (E>1.5 keV)

$k^{exp} = P^{WMo} / P^{W} = 3.0$ (2.5 keV<E<5 keV)

$k^{theor} = j^{WMo} / j^{W} = 0.92$ for mixture (W80%, Mo20%)

Appendix 2.

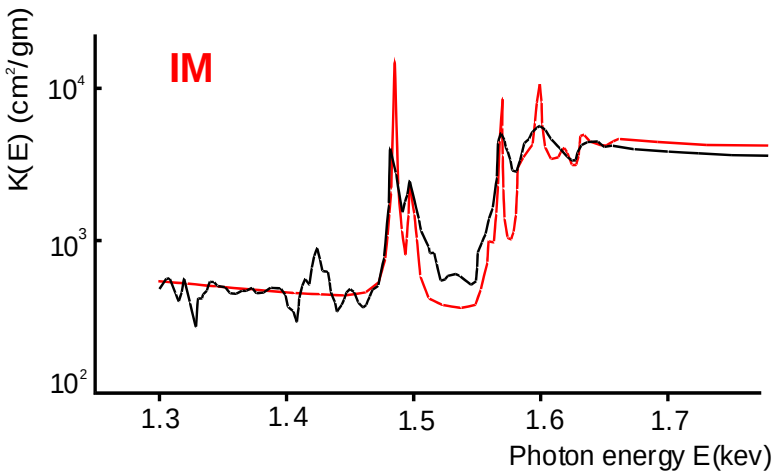

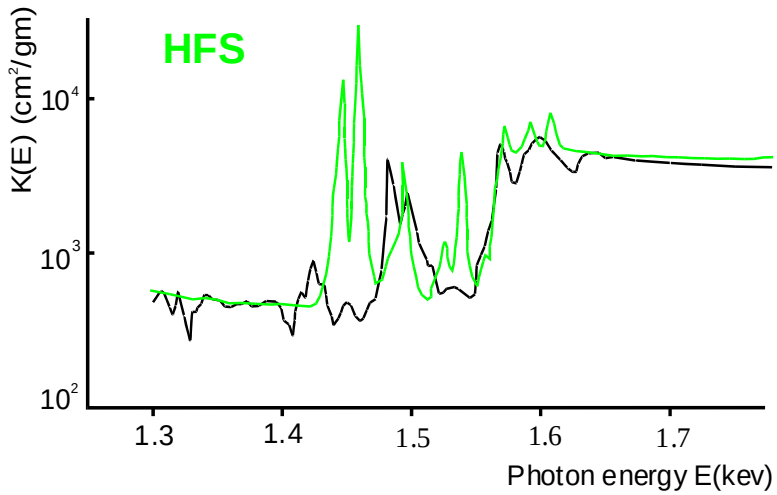

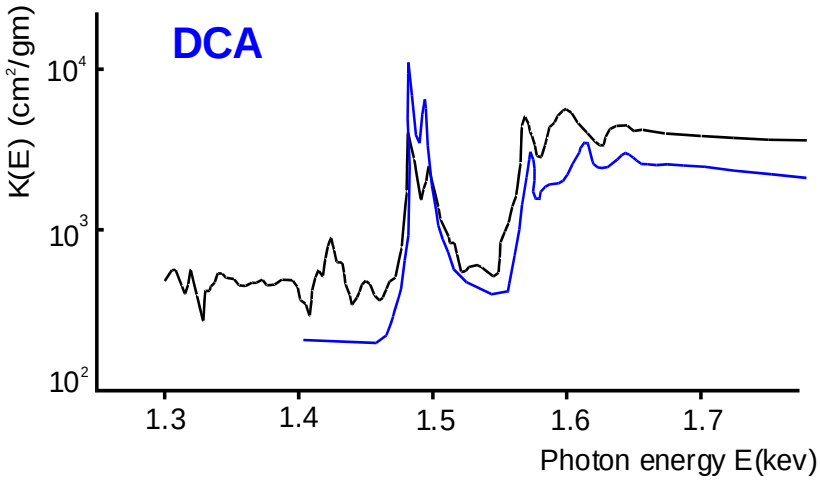

Comparison of experimental data (Davidson, S.J. et al.- black line) for the spectral coefficient of X-ray absorption and calculations (IM –red line, HFS-green line, DCA-blue line) in Al plasma at T=18eV, density 0.05 g/ccm.

Appendix 3.

The Planck mean free path (cm) calculated for NiCr and Alloy 188 at the temperature T=1 keV.

Density	NiCr	Alloy 188	k^{theor}
$0.1d^{nor}$	$1.2\ 10^{-2}$	$2.8\ 10^{-3}$	4.06
d^{nor}	$2.9\ 10^{-4}$	$2.2\ 10^{-4}$	1.38
$10\ d^{nor}$	$3.3\ 10^{-5}$	$1.8\ 10^{-5}$	1.84

$k^{theor} = j^{Alloy188} / j^{NiCr}$, d^{nor} is the normal density of material

Appendix 4.

The Rosseland mean free path (cm) calculated for different materials at the density 1 (g/ccm).

T (eV)	Au	Au50/ Gd50	Comp. 1.
200	$4.57\ 10^{-4}$	$3.29\ 10^{-4}$	$1.53\ 10^{-4}$
250	$5.01\ 10^{-4}$	$2.89\ 10^{-4}$	$1.61\ 10^{-4}$
300	$5.75\ 10^{-4}$	$3.89\ 10^{-4}$	$1.87\ 10^{-4}$